ARTÍCULO ORIGINAL

Revista de Investigación de Física **25(2)**, (May-Ago 2022)

Doi: 10.15381/rif.v25i2.23069

eISSN:1728-2977

Analysis of the magnetization for Fe and Ni ferromagnetic nanoparticles with variable geometry using VAMPIRE software

Yacu V. Alca-Ramos [*1], Juan A. Ramos-Guivar[1] and Edson C. Passamani[2]

[1] *Universidad Nacional Mayor de San Marcos, Grupo de Investigación de Nanotecnología Aplicada para Biorremediación Ambiental, Energía, Biomedicina y Agricultura (NANOTECH), Lima, Perú.*

[2] *Universidade Federal do Espírito Santo, Departamento de Física, Vitória, Espírito Santo, Brasil.*

Recibido 27 Jun 2022 – Aceptado 10 Ago 2022 – Publicado 15 Ago 2022

Abstract

The purpose of this research is to have a quantitative analysis on the temperature dependence magnetization of ferromagnetic nanoparticles (NPs), i.e., the Curie temperature (T_c), was systematically studied. The atomistic simulations were carried out using the VAMPIRE 5.0 software based on the Landau-Lifshitz-Gilbert-Heun method. The variable parameters of the simulations were damping, time step, particle geometry (spherical, cubic, and cylindrical) and particle size. We have calculated λ for Fe and Ni, in addition we have found different T_c values for each nanogeometry studied following a finite-size effect. We have found ν values for cubic NPs close to the reported values. In particular, it was observed that the T_c values for the studied geometries in the case of Fe and Ni decreases from their theoretical bulk values, for a critical particle size diameter less than 5 nm. Hence, the presented results (optimized atomistic parameters such as simulation time step, damping, and critical exponents) are the basis for advanced simulations of hybrid and complex nanostructures with perspective in biomedical and environmental applications.

Keywords: iron, nickel, critical temperature, magnetization, Curie temperature, nanoparticle.

Análisis de la magnetización de nanopartículas ferromagnéticas de Fe y Ni con geometría variable usando el software VAMPIRE

Resumen

El propósito de esta investigación es tener un análisis cuantitativo sobre la dependencia de la magnetización con la temperatura para nanopartículas ferromagnéticas, es decir, que la temperatura de Curie (T_c), fue sistemáticamente estudiada. Las simulaciones atomísticas se realizaron utilizando el software VAMPIRE basado en el método Landau-Lifshitz-Gilbert-Heun. Los parámetros variables de la simulación estudiados fueron el amortiguamiento, paso de tiempo, geometría de las partículas (esféricas, cúbicas y cilíndricas) y tamaño. Se calculó λ para Fe y Ni, además se encontró diferentes T_c para cada nanogeometría estudiada siguiendo una relación de tamaño finito. Los valores de ν para NPs cúbicas son cercanos a los valores reportados. Se observó también que los valores de T_c para las geometrías estudiadas en el caso de Fe y Ni disminuyen del valor másico teórico para un diámetro de partícula crítico menor a 5 nm. Por tanto, los resultados presentados (parámetros atomísticos simulados, como el paso de tiempo de la simulación, el amortiguamiento y los exponentes críticos) son la base para comprender simulaciones avanzadas de nanostructuras complejas e híbridos con perspectiva en aplicaciones ambientales y biomédicas.

Palabras clave: hierro, níquel, magnetización, temperatura de Curie, anisotropía, nanopartícula.

[*] 12130002@unmsm.edu.pe

Introduction

Nanomaterials exhibit chemical and physical properties that are substantially different to their respective bulk-size grains mainly due to their unique microstructure and large surface area to volume ratio. In other words, since the grains are too small (sizes in nanometric scale), a significant part of the atoms locating on the surface of the crystalline grains often determines the nanomaterial properties. Therefore, this finite-size effect gives rise to special and new properties that are not observed in their counterpart 3D-like grains (materials with ordinary grain sizes) [1].

Among the physical properties, we highlight the magnetic ones that are largely based on the phenomenon of magnetic exchange interactions that occur between magnetic moments and are purely quantum in nature [2]. However, we have to emphasize that an atom can have a permanent magnetic moment determined by the total sum of non-zero orbital and spin moment [2], and materials, in which the magnetic moments are configurated in a magnetically ordered structure, even in the absence of an external magnetic field, are called as ferromagnetic (FM), as long as their magnetic moments are pointing parallel. Nevertheless, when a material has aligned magnetic moments, but oriented in opposite directions and unbalanced in magnitude or number, giving rise to a non-zero macroscopic magnetic moment, they are called ferrimagnetic (FI). Both FM and FI materials can have significant magnetization even in the absence of an applied external magnetic field when they are in single magnetic domains. This magnetization receives the name of remanent or spontaneous magnetization. In the particular case where a material has their magnetic moments antiparallel and perfectly balanced, it will not present a spontaneous macroscopic magnetization, receiving thus the name of antiferromagnetic (AF) [3]. For all these magnetically ordered materials, there is a critical temperature T_c (Curie temperature for FM and FI) and T_N (Néel temperature for AF) where thermal fluctuations overcomes their exchange energy leading the material to a paramagnetic behavior with zero spontaneous magnetizations [4].

Currently, FM materials at nanoscale are been applied in different areas of Biomedicine (magnetic hyperthermia) and Spintronic [5, 6]. However, in nanoscale regime there are several effects that affect directly the magnetic properties and that will change the T_c value of material. Therefore, the control of this T_c value near to room temperature is desired in nanoparticle systems often suggested to be used in Biomedicine, for instance. But, before the synthesis of FM nanoparticle systems experimentally, the simulation of their magnetic properties could bring some additional advantages mainly because we can first understand theoretically their magnetic behaviors, reducing, for example, experimental setup expenses.

Regarding the simulation process, we have to mention that the VAMPIRE software (https://vampire.york.ac.uk/) is often used to simulate magnetic systems through a practical command system. The temperature dependence of magnetization, $M(T)$, of ferromagnets has been studied and simulated for different methods using Monte Carlo integration (MC), Landau-Lifshitz-Gilbert (LLG) [4], and Heisenberg mean-field theory [7]. The MC method ignores the damping parameter, but the LLG-Heun method is used for magnetic dynamic systems that evolves in time. However, it should be stressed out that few reports have been done on its applicability to find the $M(T)$ behavior in nanometric FM materials. Thus, this work focuses on using the LLG-Heun method to study the $M(T)$ behavior of FM Ni and Fe nanoparticles (NPs) materials with three different geometries and sizes ranging from 1 to 15 nm showing the influence of the finite-size effect on the FM Ni and Fe nanograins.

Theoretical description of the atomistic simulations

- Temperature dependent magnetization

The magnetization M is defined as the magnetic dipole moment density in the direction of the magnetic field, but we have used for this work the dimensionless quantity known as relative magnetization, $m = M/M_s$, whose values oscillate between 0 and 1 in all graphics, while for discussions, $M(T)$, was used the following approximations.

The Curie-Bloch equation (1), in the classical limit, was used to find T_c [8], and the aproximation for finite size scalling law Equation (2) [9].

$$m(T) = \left(1 - \frac{T}{T_c}\right)^{\beta} \tag{1}$$

$$\left(\frac{d_0}{D}\right)^{\frac{1}{\upsilon}} = \left(\frac{T_c(\infty) - T_c(D)}{T_c(\infty)}\right) \tag{2}$$

where ν is the phenomenological shift exponent, $D(nm)$ is the length of the NPs geometries, $T_c(\infty)$ is the bulk Curie Temperature, and d_0 is the microscopic length close in value to the single unit cell in the lattice structure of the FM material [8]. For this work, we have used the following approximation by means of a polynomial fit in ORIGIN 9.0 (https://www.originlab.com/) software denoted by:

$$T_c(D) = T_c(\infty)\left(1 - \left(\frac{A}{D}\right)^{B}\right) \tag{3}$$

where A and B are critical exponents that we must find for each geometry. Error ranges in T_c curves were found to be equal to 2-5 % for the tested nanogeometries.

- Software VAMPIRE and the atomistic spin model

The software VAMPIRE works with the atomistic spin model, which operates in the follow manner: It creates a crystalline structure of roughly desired shape; then, every atom is assigned to the desired material with physical properties such as damping, atomic spin moment, exchange energy, features that often found in 3D-like materials. The Hamiltonian for the simulated system is given by [4].

$$H = -\sum_{i \neq j} J_{ij} S_i S_j \; - k_2 \sum_i S_z^2 \qquad (4)$$

where J_{ij} describes the contributions of exchange interactions between magnetic moments of the nearest neighbors, S_z is the uniaxial anisotropy, k_2 the anisotropy constant, and S_{ij} is the unit vector that describes the orientation of the local spin moment. For most FM materials, the exchange energy is usually the dominant contribution for the Hamiltonian. In addition, we would like to remember that FM materials have $J > 0$, while AF ones $J < 0$.

The Hamiltonian describes the energy of the system but does not give information about the dynamics of the spin. For this, the LLG equation is used, which describes the dynamics of the spin and is given by [4]:

$$\frac{\partial S_i}{\partial t} = -\frac{\gamma}{1+\lambda^2}\left[S_i \times B_{eff}^i + \lambda S_i \times \left(S_i \times B_{eff}^i\right)\right] \qquad (5)$$

where γ is the magnetic spin ratio, B_{eff}^i is the effective (net) magnetic field at each spin, and λ is a phenomenological damping constant, which is an intrinsic property of the material. VAMPIRE software has a number of functions dedicated to generate atomic systems within the nearest neighbor approximation. The LLG equation is numerically integrated using the Heun numerical scheme, which simulates the evolution of the spin system with time (spin dynamics) [4].

Results and discussion

Determination of damping parameter for FM Fe NPs

Fe NPs were first studied in the absence of external magnetic field, and it was performed with the LLG dynamics method that obeys a description of the precision movement of magnetization in a solid, this method also allows describing the dynamics of small magnetic elements. For this first case, we considered a temperature of 50 K and time-equilibrium step around 15000 s, which is the number of steps it takes for the spins to fluctuate to a thermal equilibrium state, until it reaches the critical temperature (this step value was previously optimized).

We then proceeded also to optimize the λ parameter using a size of 7 nm for the Fe NPs with cubic geometry using ab initio exchange parameters given by [4]. As it is shown in Figure 1, different values of λ were found. In addition, one has to comment that each value of damping was tested for a time-step that ranged from 1.0×10^{-15} s to 5.0×10^{-15} s.

As it can be observed from Figure 1, the damping value affects drastically the T_c value. In addition, the time-steps (for a fixed damping value) also influence the $M(T)$ behavior. In particular, looking the simulated data of Figure 1 (b) and (c), we can see that for the time-step value of 1.0×10^{-15} s the curve (light blue color) does not lose magnetization and is apparently "smooth" as the temperature increases, so the λ we are looking for must be in that interval. Then, having already a defined time-step, we proceeded to find the T_c for different λ values ranging from 0.1 to 1.0, as shown in Table 1. Then, the reference value for the λ was 0.2.

λ	0.1	0.2	0.3	0.4	0.5
T_c (K)	1818.5	1027.6	1050.3	1096.9	1080.9
λ	0.6	0.7	0.8	0.9	1.0
T_c (K)	1073.1	1111.1	1128.2	1118.4	1101.2

Table 1: T_c values obtained for diferent dampings.

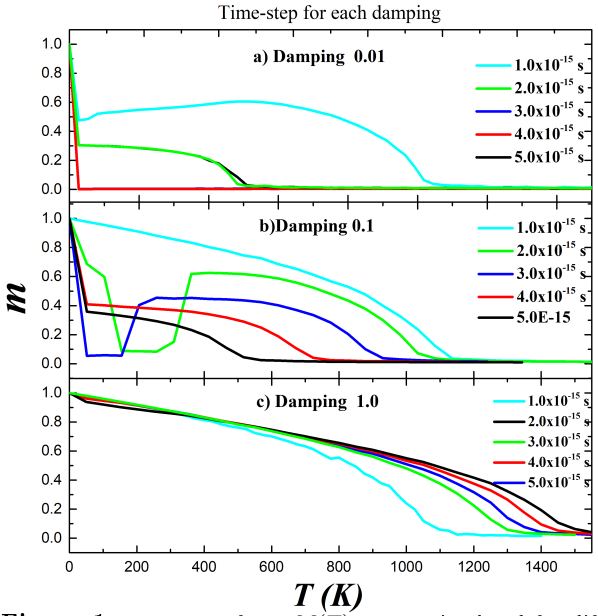

Figure 1: Behavior of the $M(T)$ curves simulated for different dampings [0.01(a), 0.1(b), and 1.0(c)] for FM 7 nm Fe NPs with cubic-like geometry. For each damping, the time-step behavior of the $M(T)$ curves are also shown.

Simulations performed for cubic, spherical, and cylindrical geometries of FM Fe NPs

After the determination of main parameters of the simulation for the FM Fe NPs, we have now changed their sizes and shapes (we call as NPs including particles with cylindrical geometry to simplify our discussion). In particular, we started with cubic and spherical geometries for the Fe NPs cubic and spherical geometries for the Fe NPs, see Figure 2(a) and 3 (a) . It should also be mentioned that while for the cubic geometry the hypothetical material lenghts (x, y and z axes) increase uniformly from 1 to 15 nm, the spherical NPs have their radius (r) also gradually increased in the same interval.

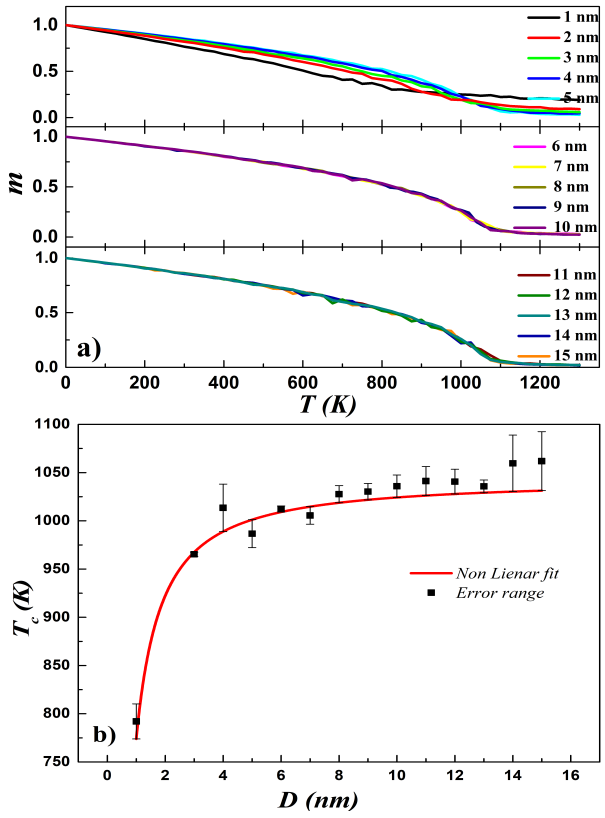

Figure 2: Behaviors of simulated normalized $M(T)$ curves obtained for 1-15 nm FM Fe NPs with cubic geometry (a) and the dependence of the T_c with NP lenght (D is the particle dimension)(b).

As it can be seen in Figure 2 (b) and Figure 3 (b), the T_c value increases as the nanoparticle dimensions increase for the cubic geometry, although the points obtained are far from the theoretical fit obtained from the Equation 2. On the other hand, for the cylindrical geometry the dimensions of the z axis were varied from 1 nm to 15 nm maintaining a constant radius of 4 nm.

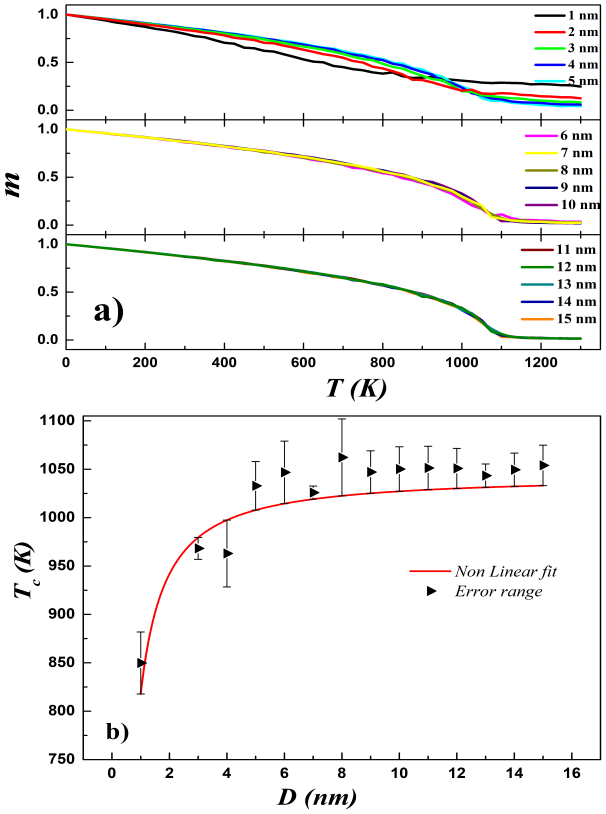

Figure 3: Behaviors of simulated normalized $M(T)$ curves obtained for 1-15 nm FM Fe NPs with spherical geometry (a) and the dependence of the T_c with NP lenght (b) as a shown.

On the other hand, Figure 4(a) and (b) shows the behaviors of $M(T)$ and $T_c(D)$ (D is the NP lenght) for Fe NPs with cylindrical shape. It can be seen that unlike the cubic and spherical geometries, in this case the larger the sample size favors T_c fluctuates below the theoretical setting. T_c increases as the dimensions of the nanoparticle increases, although the values obtained are in agreement with the theoretical fit performed with the modified Equation 6.

$$T_c = 1043 \times \left(1 - \left(\frac{A}{D}\right)^B\right) \tag{6}$$

where A,B are fit parameters obtained with ORIGIN 9.0 software and D is the size of NP.

$$T_c = 1043 \times \left(1 - \left(\frac{A}{\sqrt[3]{D}}\right)^B\right) \quad (7)$$

The parameters obtained by a nonlinear fitting using Equations 6 and 7 are in the Table 2.

For cylindrical geometry, the function 6 was modified because only one dimension was changed, but radius of transversal section was kept fixed while the lenght z-axis was modified, obtaining the Equation 7

	A	B	ν
Cubic geometry	0.310	1.156	0.865
Spherical geometry	0.264	1.152	0.868
Cylindrical geometry	0.069	0.937	1.067

Table 2: Critical A and B values for different Fe morphologies.

In general, $T_c(D)$ data for the three shapes (cubic, spherical and cylindrical) show a strong reduction on T_c values for sizes below 5 nm, indicating that this could be the limit size where the finite-size effect starts to be relevant on the T_c values of FM Fe NPs.

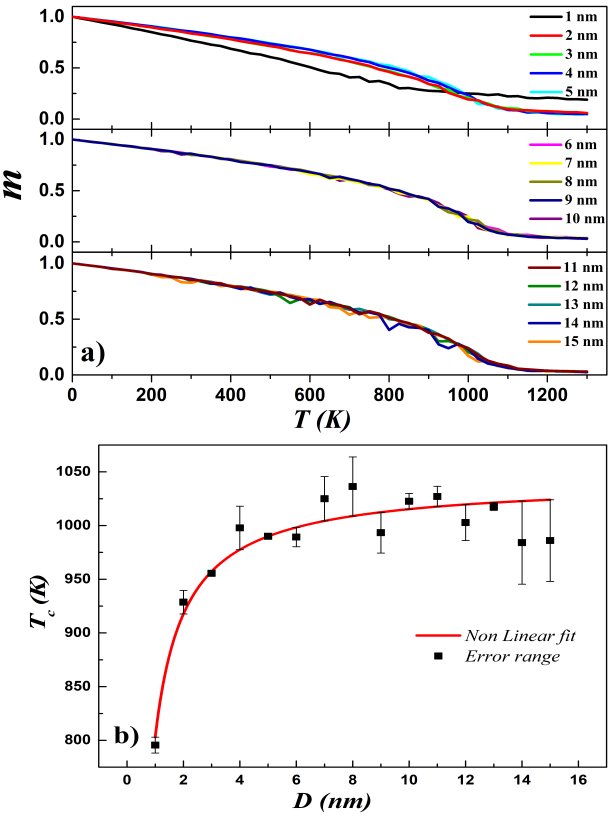

Figure 4: (a) Behaviors of simulated normalized $M(T)$ curves obtained for FM Fe NPs with cylindrical geometry. (b) Dependence of the T_c with NP lenght (D).

Determination of damping parameter for FM Ni NPs

Similar procedures used for FM Fe NPs were also employed here for FM Ni NPs. Thus, atomistic simulations were made for a 7 nm cubic NPs, and with damping values (λ parameter) equal to 0.01 (a), 0.1 (b), and 1.0 (c) and with different values of time-steps, as indicated in Figure 5. The optimum λ value occurs between 0.01 and 0.1, because λ= 0.01 favors $M(T)$ curves with fasting decay and with low slope, while the λ = 0.1 results in $M(T)$ curve that does not decay as fast as the previous ones, but have deeper slopes, thus matching with behaviors expected for theoretical models. For the λ = 1, the T_c is very high. It is also observed in T_c data displayed in Table 3 that the greater the value of the time-step lower is the T_c values for these two cases (0.01 and 0.1). We would like to mention that caution should be taken for small λ values such as 0.01, when the simulation is done with a time-step greater than 3.0×10^{-16} s, because the atomic arrays will lose abruptly near T = 0 K. In other words, this behavior does not correspond to the theoretical model. Therefore, an aceptable value of the time-step has an upper limit for each λ, as suggested the $M(T)$ behaviors shown in Figure 5. All simulations had loop and time equilibration steps values of 2000 s.

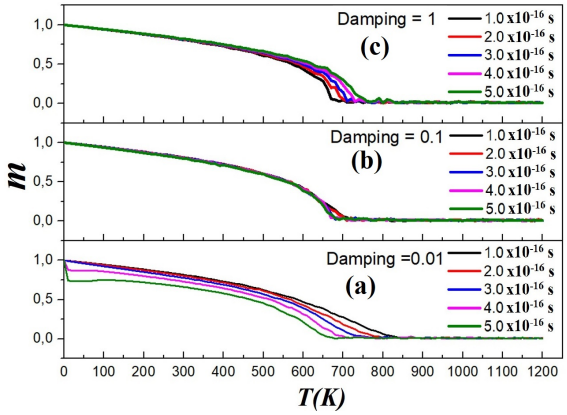

Figure 5: Behaviors of simulated normalized $M(T)$ curves performed for the FM Ni NPs with size of 7 nm and cubic geometry. The $M(T)$ curves were simulated using different damping (λ) values [0.01 (a), 0.1 (b), and 1.0 (c)] and time-steps, as indicated also in the Figure.

		λ		
		0.01	0.1	1
Time-step (s)	1.0×10^{-16}	728 K	686 K	660 K
	2.0×10^{-16}	692 K	628 K	679 K
	3.0×10^{-16}	653 K	676 K	689 K
	4.0×10^{-16}	622 K	662 K	705 K
	5.0×10^{-16}	620 K	652 K	719 K

Table 3: T_c for diverse configurations of λ and time step.

Hence, λ values between 0.01 and 0.1 were analyzed, finding that the value of 0.03 corresponds to a T_c value near to the FM bulk-like Ni material (631 K), as shown in Table 4.

λ	0.02	0.03	0.04	0.05
T_c (K)	634	633	639	638
λ	0.06	0.07	0.08	0.09
T_c (K)	647	642	648	648

Table 4: T_c values obtained varying damping (λ) and time-step parameters for FM Ni NPs with cubic geometry.

Simulations for cubic, spherical, and cylindrical geometries for FM Ni NPs

The behaviors of simulated normalized magnetization ($M(T)$) curves were systematically studied for FM Ni NPs with different geometries as also conducted for FM Fe NPs previously presented.

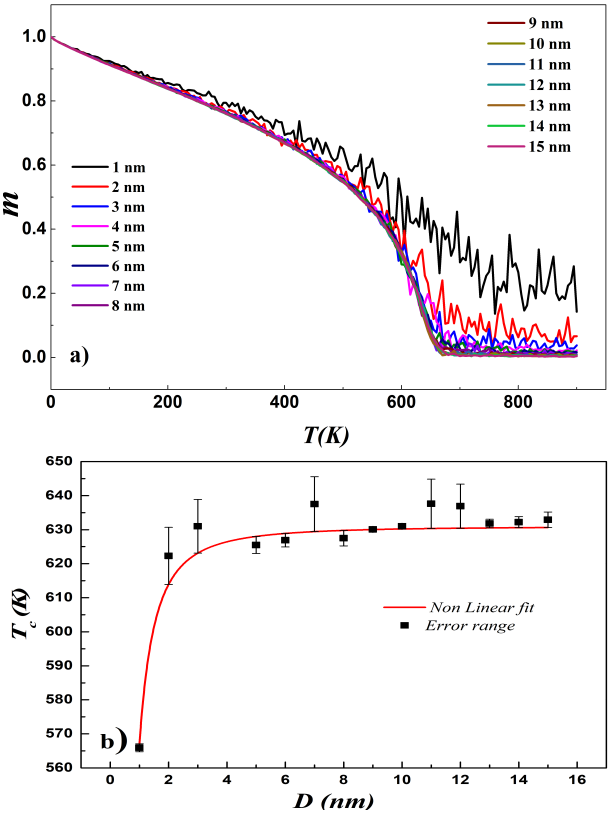

Figure 6: Behaviors of simulated normalized magnetization [$M(T)$] for FM Ni NPs with cubic (a) geometry and the dependence obtained for different sizes (dimension D of the NPs) (b).

For cubes and spherical NPs, see Figure 6(a) and 7(a), the edge and diameter ranged from 1 to 15 nm, respectively. In the case of the cylinder, a diameter of 3 nm was fixed while the length on the z axis was changed in a range between 3 nm and 45 nm. The chosen time-step was 4.8×10^{-16} s because it was the upper limit for λ equal to 0.03. The results are shown in Figures 6,7 and 8.

The data of T_c obtained from the simulated $M(T)$ curves as a function of particle lenght (D) are respectively shown in Figure 6(b), Figure 7 (b) and 8(b) for cubic, spherical and cylindrical geometries, respectively. These $T_c(D)$ data were fitted using the data of T_c obtained from the simulated $M(T)$ curves as a function of D and they are respectively shown in Figure 6(b), 7(b), and 8(b) for cubic, spherical, and cylindrical geometries, respectively. These $T_c(D)$ data were fitted with ORIGIN 9.0 software using a non-linear fit with the following function for FM Ni NPs with cubic [6(b)] and spherical [7(b)] geometries (Equation 8 was used for these cases).

$$T_c = 631 \times \left(1 - \left(\frac{A}{D}\right)^B\right) \tag{8}$$

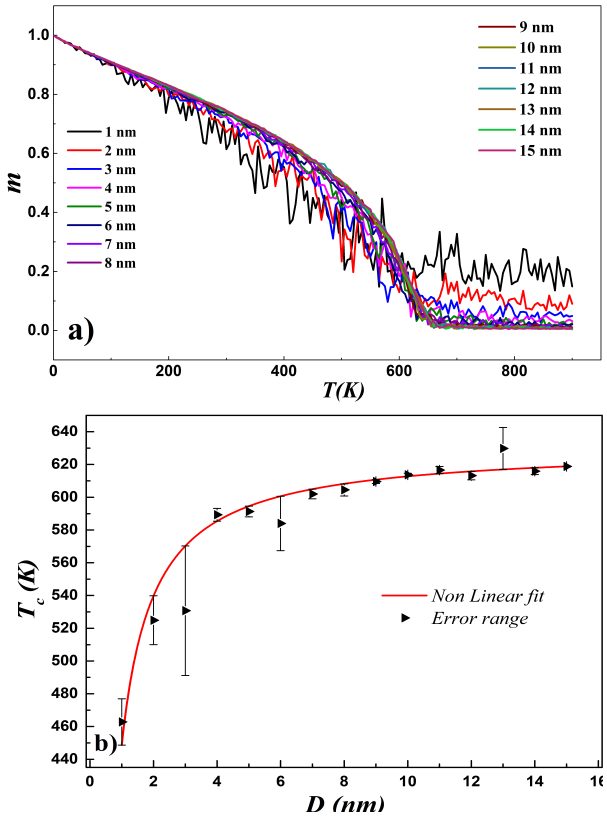

Figure 7: Behaviors of simulated normalized magnetization [$M(T)$] for FM Ni NPs with spherical (a) geometries and the dependece obtained for different sizes (b).

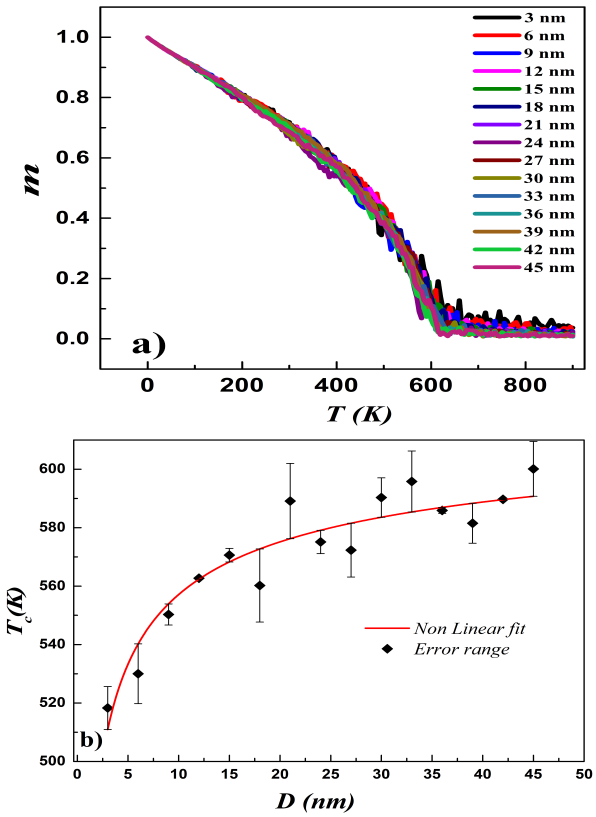

Figure 8: Behaviors of simulated normalized magnetization $[M(T)]$ for FM Ni NPs with cylindrical geometry (a) obtained for different dimension D of the NPs. Dependence of the T_c as a function of NP size $[T_c(D)]$ are also shown in (b) for cylindrical geometry.

For cylindrical geometry,see Figure 8(a),the function was modified because only one dimension was changed because the radius of transversal section was fixed while the lenght (z-axis) was modified in the simulation, i.e., the Equation 9 was used.

$$T_c = 631 \times \left(1 - \left(\frac{A}{\sqrt[3]{D}}\right)^B\right) \tag{9}$$

The values of A and B obtained from atomistic simulations are reported in Table 5:

	A	B	ν
Cubic geometry	0.300	1.903	0.525
Spherical geometry	0.288	1	1
Cylindrical geometry	0.016	0.403	2.481

Table 5: Critical A and B values for different FM Ni NP morphologies.

Conclusions

- Finding an adequate λ for the atomistic simulation is crucial and important, as shown in Figure 1 and 5, this parameter has a great influence on the behavior of the simulated normalized $M(T)$ curves for both FM Fe and Ni NPs. Specifically, it was shown that damping values smaller than 1.0 favor an abrupt reduction of the magnetization.

- Another important factor to take into account for simulations is the value of the time step, which is correlated with damping and with the adequate calculation of the T_c.

- The results shows that the T_c increases as the NP size of the sample increases and its behavior is given by the fitting curve until that behaves asymptotically with respect to T_c of bulk. Particle sizes smaller than 5 nm favor reduction of T_c due to the finite-size effect.

- The behavior of a magnetic system close to a critical phase transition leads to a magnetization reduction from FM to paramagnetic state, such as Fe and Ni. The various critical parameters resulting from such a phenomenon are the critical specific heat exponent α, the spontaneous magnetization exponent β, the initial susceptibility exponent γ, and the critical spin correlation length exponent ν, that last has not been directly calculated for these elementary FM due to their high T_c values, and in case of atomistic simulations. Therefore, in this work we tried to address this problem by analyzing this parameter for different nanogeometries. Hence, the ν values obtained of 0.865 for Fe and 0.525 for Ni in cubic geometries can be highlighted in both cases, which are close to the values described in [10], reporting finding values of 0.703 for fcc systems and 0.706 for bcc systems, respectively.

Acknowledgments

The authors thank PROCIENCIA for financial support via the multidisciplinary project FONDECYT N° 177-2020. Edson C. Passamani would also like to thank Universidade Federal do Espírito Santo (UFES), Fundação de Amparo á Pesquisa e Inovação do Espírito Santo (FAPES), and Conselho Nacional de Pesquisa (CNPq) for their financial supports.

References

[1] C.C. Koch, Nanostructured Materials: Processing, Properties and Applications. Elsevier Science, (2007).

[2] B.D. Cullity and C.D. Graham, Introduction to Magnetic Materials. New Jersey, second edition Wiley, (2011).

[3] C. Kittel, Physical theory of ferromagnetic domains. Reviews of Modern Physics, 21(4):541–583, (1949).

[4] R. F. L. Evans, W. J. Fan, P. Chureemart, T. A. Ostler, M. O. A. Ellis, and R. W. Chantrell. Atomistic spin model simulations of magnetic nanomaterials, Journal of Physics: Condensed Matter, 26(10):103202, (2014).

[5] E. Kita, T. Oda, T. Kayano, S. Sato, M. Minagawa, H. Yanagihara, M. Kishimoto, C. Mitsumata, S. Hashimoto, K. Yamada, and N. Ohkohchi, Ferromagnetic nanoparticles for magnetic hyperthermia and thermoablation therapy, Journal of Physics D: Applied Physics, 43(47):474011, (2010).

[6] D. Anbuselvan, S. Nilavazhagan, A. Santhanam, N. Chidhambaram, K.V. Gunavathy, Tansir Ahamad, and Saad M. Alshehri, Room temperature ferromagnetic behavior of nickel-doped zinc oxide dilute magnetic semiconductor for spintronics applications, Physica E: Low-dimensional Systems and Nanostructures, 129:114665, (2021).

[7] C. Penny, A. R. Muxworthy, and K. Fabian. Mean-field modelling of magnetic nanoparticles: The effect of particle size and shape on the curie temperature. Physical Review B, 99(17), (2019).

[8] J. A. Ramos-Guivar, C. A. Tamanaha-Vegas, F. J. Litterst, and E. C. Passamani, Magnetic simulations of core@shell ferromagnetic bi-magnetic nanoparticles: The influence of antiferromagnetic interfacial exchange, Nanomaterials, 11(6):1381, (2021).

[9] Hovorka, O., Devos, S., Coopman, Q., Fan, W. J., Aas, C. J., Evans, R. F. L., Chen, X., Ju, G., and Chantrell, R. W. The Curie temperature distribution of FePt granular magnetic recording media. Applied Physics Letters, 101(5), 052406, (2012).

[10] Chen, K., Ferrenberg, A. M., and Landau, D. P. (1993). Static critical behavior of three-dimensional classical Heisenberg models: A high-resolution Monte Carlo study. Physical Review B, 48(5), 3249–3256, (1993).